sciendo

ACTA CHEMICA IASI, **27_2**, 287-302 (2019)

DOI: 10.2478/achi-2019-0018

STRUCTURAL AND OPTOELECTRONIC PROPERTIES OF ZINC SULFIDE THIN FILMS SYNTHESIZED BY CO-PRECIPITATION METHOD

V.H. Choudapur[a], S.B. Kapatkar[a*] and A.B. Raju[b]

[a]*Department of Physics, B.V.B. College of Engineering and Technology, Vidyanagar, Hubli, 580 031, Karnataka, India*

[b]*Department of Electrical and Electronics Engineering, B.V.B.College of Engineering and Technology, Vidyanagar, Hubli, 580 031, Karnataka, India*

Abstract: Wide bandgap Zinc Sulfide nanocrystals are prepared by a simple co-precipitation method at different precursor concentrations. The influence of sulphur concentration in Zinc sulfide on morphological, optical and electric properties is found to be significant. The Zinc Sulfide nanomaterial was prepared using low-cost starting materials and deionised water as the solvent. As synthesized Zinc Sulfide nanocrystals were analyzed using X-ray diffraction (XRD), Energy Dispersive Spectroscopy (EDS) analysis, UV-Visible Spectrophotometry, Photoluminescence (PL), Scanning electron Microscopy (SEM), Ellipsometry techniques and electric conductivity measurements. XRD patterns revealed that ZnS nanocrystals are polycrystalline, cubic phase with (111) preferred orientation. The obtained crystallites have sizes in the range of 5 to 11 nm. EDS pattern confirms the purity of the films. From optical absorption measurements, it is clear that the direct energy gap decreases from 5.2 to 4.4eV with the increase in sulphur concentration in ZnS and exhibit large quantum confinement effect. Ellipsometry was used to determine the optical constants and film thickness. The films deposited on ITO – coated glass was used to record the *IV* Characteristics of the films by two probe method. The wide-bandgap, conducting materials have applications in optoelectronic devices such as high-frequency UV detectors and thin-film solar cells.

***Keywords*:** ZnS thin films, wide bandgap, low- cost precursors, spin coating, preheating

[*] S.B.Kapatkar, *e-mail:* sbkapatkar@bvb.edu

Introduction

Semiconducting nanoparticles have been studied widely due to their interesting size-dependent optoelectronic properties. Nanostructured materials have sizes in the 1–100 nm range, which makes them attractive for improving material and device performance in several applications[1]. Chalcogenide semiconductor nanomaterials play an essential role in contemporary nanoelectronics. II-VI group semiconductors (Zinc and Cadmium chalcogenides) are wide bandgap semiconductors and transparent materials which have significantly contributed to the development of thin-film device technology. Wide-band gap materials (2 to 4 eV) exhibit a significant quantum confinement effect. The optoelectronic properties of a nano semiconductor mainly depend on the crystallite size, morphology and their optical response which can be tuned widely through chemical synthesis methods of nanomaterials by varying the reaction conditions like precursor concentrations, pH, temperature, and length by using various types of capping agents during synthesis.[1-4]

Wide bandgap transparent Conductors (TCs) play an important role in present nanodevices. The TCs exhibit a combined effect of transparency and electric conductivity, which has generated both fundamental and technical importance in many applications. As a result, these II-VI semiconducting materials have been seen as a better choice for many potential applications such as transparent electronics, display devices, thin-film solar cells, electroluminescent devices, lasers and chemical/biological sensors etc.[3, 4]

In recent years, ZnS thin films have been investigated intensively due to their interesting optoelectronic properties. Zinc Sulfide is a eco-friendly semiconductor material due to its non-toxic nature and low-cost

starting materials; it also displays high refractive index (2.4), high direct energy gap and high exciton binding energy of 40 meV as well as n-type conductivity. ZnS exhibits both cubic phase (*Eg* ~3.72 eV) and hexagonal phases (*Eg* ~3.77 eV) and possesses transparency over wide range of solar spectrum.[1] It is useful, as an antireflection coating or a buffer layer in heterojunction thin-film solar cells.[4] ZnS is widely used as a passivating layer for core-shell structures in several semiconductors to enhance their stability and fluorescence properties. They are also used as host material to get doped semiconductor nanocrystals.[3] Recently several works have been carried out to develop buffer layers free of cadmium for CIGS thin-film solar cells and to find an alternative eco-friendly material for the buffer layer. Due to the wider bandgap of ZnS, it transmits more energetic light photons to the absorber layer of the junction and enhances the emission in the visible region as compared to CdS. Therefore ZnS buffer layers, being inexpensive and non-toxic, can replace the Chemical bath deposited CdS in CIGS solar cells.[3,4] With these interests, various methods have been developed to grow ZnS nanomaterial such as chemical Silar method,[5] Chemical bath deposition,[6,1] Co-precipitation method[7], colloidal method,[8,9] thermal evaporation,[10] Sputtering,[12] etc. Among these, Co-precipitation method of synthesis and deposition using spin coating has been considered as one of the cost-effective deposition techniques.[13]

In the present investigation, ZnS nanomaterials with wide bandgap and high transparency have been prepared by a simple co-precipitation method without using capping agents. The effect of sulphur concentration on optoelectronic properties was studied.

Experimental details

Sample preparation

Zinc acetate [$Zn(OOCCH_3)_2$], Sodium sulfide flakes purified [Na_2S] of AR grade purchased from S.D. fine chem. limited-India. Deionized water is used as solvent and all the chemicals were used without further purification. ZnS NCs are synthesized at RT in aqueous medium by mixing 0.5 M of Zinc acetate and 0.5 M sodium sulfide, with continuous stirring on magnetic stirrer of 1000 rpm. The pH of the solution is in the range 5 to 6. The reaction is carried out at 60^oC for 1hr in open conditions. ZnS nanocrystals so formed are washed repeatedly by alternative ultrasonication and centrifugation using the solvents. Finally the ZnS crystals were separated and dried at room temperature. ZnS nanoparticles prepared at different molar ratios of Zn^{+2}: S^{2-}, 0.5 M/0.5 M, 0.5 M/0.75 M and 0.5 M/1 M were labeled as S1, S2 and S3 samples and synthesized under above mentioned experimental conditions. Spin Coating machine (NXG-P1, APEX India) is used to prepare thin films of S1, S2 and S3. The glass slides are cleaned by standard procedure before the deposition of thin films. Attempts were made to deposit films of all the samples at different speeds of spin coating at room temperature to optimize coating conditions. Adherent and uniform thickness spin-coated ZnS thin films obtained for 2000 rpm for 30 seconds. The spinning to preheating procedure was repeated for eight times at 50°C for 5 minutes.

Characterization techniques

The XRD analysis was conducted using an X-ray powder diffractometer (Bruker AXS D8 Advance, STIC, Cochin) with CuKα radiation (1.5406 A^0). UV-Visible Absorption spectra were recorded in the

range of 200-800 nm using a UV-Vis-NIR Spectrophotometer V-670 Jasco International, and PL spectra were recorded using a Fluorescence spectrophotometer Hitachi, Japan. The SEM inspection appealed to a STIC Cochin, (JEOL Model JSM -6390LV) equipment, the chemical composition analysis is carried out at the Centre for Nano Science and Engineering (CeNSE - IISc, Bangalore). Film thickness was measured using a Bruker Ellipsometer (M-2000 U, J.A. Woollam Co. Inc.), A Keithley 617 programmable electrometer was used to record the current - voltage curves on films at normal room temperature by two probe method.

Results and Discussion

X-ray diffraction studies

Figure 1 shows the X-Ray diffraction (XRD) pattern of the as-prepared nanocrystals measured in the scanning range 0 to 90^0. Phase identification of the material was carried out using standard JCPDS card No. 05-0566. Three intense broadened diffraction peaks can be observed, located at 2θ values of 28.74^o, 48.05^o, and 56.46^o, indexed as (111) (main Peak), (220) and (311) reflections of cubic ZnS, respectively with major deviation along (111) direction. The lattice constant of the ZnS crystallites was determined from the XRD patterns using the formula (1)

$$d_{hkl} = \frac{a}{\sqrt{h^2+k^2+l^2}} \qquad (1)$$

where h, k, l stand for Millar indices. The lattice parameter '*a*' is calculated as 5.37 A^0, almost the same as the standard value 5.42 A^0 as per table 1. The XRD peaks are broadened due to nanocrystalline nature of samples. The Debye Scherer equation is used to calculate the average crystallite size, D.[14] The quantity δ represents the dislocation density which represents the amount of defects in the lattice, and its value was found using the formula 2

$$\delta = 1/D^2 \quad (2)$$

while the strain (ε) in the film is estimated according to formula 3[14]

$$\epsilon = \beta cos\theta /4 \quad (3)$$

where β stands for FWHM (full width at half maximum) in radians, and θ is the Bragg angle. The calculated structural parameters are and presented in table 2. The crystallite size is dependent on precursor concentrations. The crystallite size decreases with an increase in Zn^{+2}:S^{2-} molar ratio, i.e., as the sulphur concentration increases the crystallinity and the crystallite size of the ZnS increases. At the higher concentrations of sulphur, due to availability of Zn^{+2} and S^{2-} ions, more nanoparticles are formed, and hence particle size is larger. Hence by changing the molar ratio or sulphur concentration, the particle size can be controlled.[15]

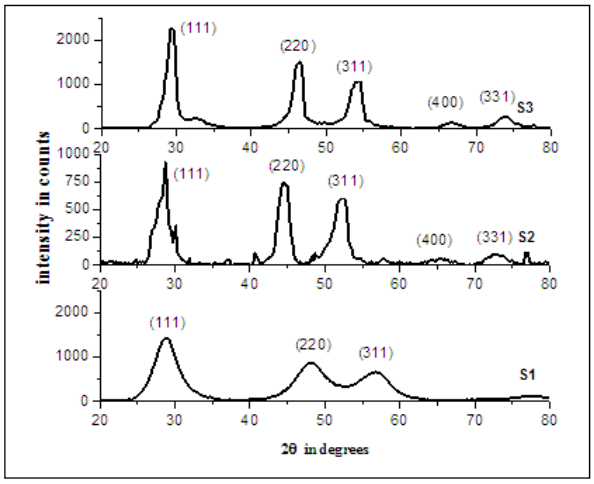

Figure 1. XRD patterns of S1, S2, and S3 samples.

The particle size can also be controlled by changing the pH of the reaction mixture. There is an increase in the particle size from 1.2 to 1.5 nm with an increase in pH of the solution from 4 to 12, resulting in a large quantum confinement effect. The ZnS nanocrystals were prepared in methanol medium without adding any capping agent.[13]

Table 1. Lattice constants calculated from XRD pattern

Peak 2θ in deg				'd' in obtained A^0			'd' in A^0 Standard	Lattice Parameter a in A^0
S1	S2	S3	(hkl)	S1	S2	S3		
28.8	28.5	28.5	(111)	3.10	3.12	3.12	3.12	5.37
48.0	47.2	47.5	(220)	1.89	1.92	1.91	1.91	5.37
56.9	56.1	56.4	(311)	1.62	1.63	1.62	1.63	5.37

Table 2. Structural parameters

sample	Plane	FWHM(β) in radians	D in nm	δ in $(m)^{-2}$	Strain 'ε'
S1	(111)	0.030	4.82	$0.043x10^{14}$	$7.48x10^{-3}$
S2	(111)	0.017	8.51	$0.014x10^{14}$	$4.24x10^{-3}$
S3	(111)	0.014	10.68	$0.876x10^{14}$	$3.38x10^{-3}$

The average size ZnS nanocrystals prepared by the hydrothermal method was of 13.08 nm, 14.57 nm and 28.06 nm at different precursor concentrations of 1:0.7, 1:1 and 1: 1.3 using zinc sulphate and sodium sulfide as starting materials at 220 $^{\circ}$C.[16] For comparison, the particle sizes of 25.57, 22.74 and 34.08 nm, respectively were reported[17] at a different annealing temperature of films of 300 $^{\circ}$C, 400 $^{\circ}$C and 500 $^{\circ}$C prepared by magnetron sputtering method.

Energy dispersive spectroscopy (EDS) analysis

Figure 2 shows EDS spectra of S1, S2 and S3. The spectra of all samples S1, S2 and S3 show the main peaks of both Zn and S of ZnS nanomaterial synthesized at different sulphur concentrations. Also low

peaks of O and C (Oxygen and Carbon) are impurity peaks. The peaks of C, O may originate, respectively from the surrounding air atmosphere and the unreacted metal salts.

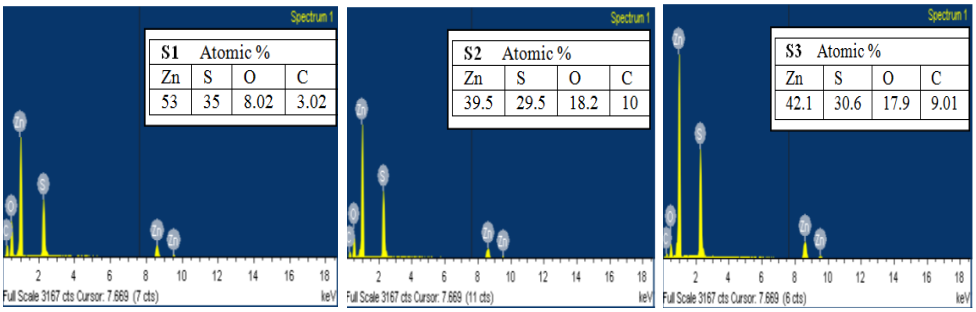

Figure 2. EDS graphs for S1, S2, and S3.

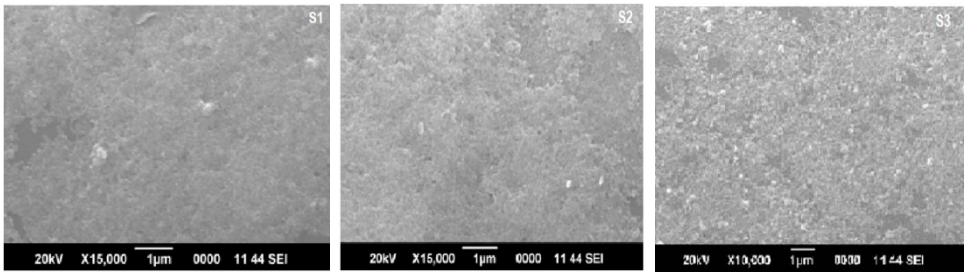

Figure 3. SEM images for S1, S2, and S3.

Also, carbon contamination may be due to the carbon tape used while performing EDS analysis. The results of both SEM and XRD analyses showed that ZnS nanoparticles were of high purity.

Scanning electron microscopy

Figure 3, exhibits surface morphology of as-synthesized ZnS thin films S1, S2 and S3 prepared at different precursor concentrations. The films exhibited uniformly distributed particles with granular shapes as well as particle agglomerations. Agglomeration prevents further disintegration into smaller particles. The grains are agglomerated. The real particle size cannot be determined from the SEM images due to the lesser magnification.[7]

Optical Absorption Analysis

Optical absorption spectra of ZnS nanocrystals were recorded in the wavelength range between 200 and 500 nm, as shown in figure 4 as normalized curves. Maximum absorption is observed in the short wavelength region that is in UV region and then decreases with increasing wavelength. Absorption edges are formed at 238 nm, 258 nm and 280 nm for S1, S2 and S3 samples respectively as summarized in table 3. In the neighborhood of 250 nm, the absorption is prominent resulting in quantum confinement effect. As compared to bulk ZnS crystals a blue shift of the absorption edge from 320 nm to 250 nm is registered. Thus, the optical band gap has been enlarged for all the three samples. The extent of energy absorption of a semiconductor is determined by the absorption coefficient of the material. Optical absorption coefficient 'α' of nanomaterials was obtained using the expression 4,

$$\alpha = 2.303 \times \frac{A}{t} \quad (4)$$

where 't' is the width of the sample under illumination, A is absorbance given by equation 5,

$$A = log \frac{I_0}{I} \quad (5)$$

where I_o and I denote the intensity of incident and transmitted light, respectively. The relation between 'α' and the energy of incident light 'hv' is given by equation 6,

$$(\alpha hv)^n = B(hv - E_g) \quad (6)$$

where E_g is the optical band gap, B is constant and n = 2 for semiconductors with direct bandgap.[14] The graph of $(\alpha hv)^2$ against incident photon energy (hv) is used to calculate the E_g. The linear portion of the graph is extrapolated up to the x-axis; the intersection value gives E_g (Figure 5). From the graph, the optical band gap is found to be 5.20 eV, 4.81 eV and 4.44 eV for S1, S2, and S3 samples respectively as summarized in table 3.

The bandgap increased with decrease in sulphur concentration, due to a decrease in particle size and large quantum confinement effect. The bandgap of 4 eV was reported for zinc sulfide material at 0.5 M/1M concentration ratio by precipitation method at 80 ^{0}C,[4] which is lesser than the value reported in this paper at the same concentration. Very wide-bandgap 4.9 to 5.6 eV are reported by non-aqueous method at different pH values and synthesized by the same co-precipitation method.[13] The band gaps of 3.76 eV, 3.74 eV and 3.65 eV were reported[15] at different precursor concentrations of 1:0.7, 1:1 and 1:1.3 respectively prepared by hydrothermal method at 220 ^{0}C. Here also the band gap was increased with increase in Zn/S ratio. These values are comparatively lesser than the values reported in this paper which may be due to the different methods and different solvent used for the synthesis. Further using bandgap energy, the crystallite size can be calculated using the Brus equation 7.[2]

$$E_{g(nano)} - E_{g(bulk)} = \frac{h^2}{8r^2}\left[\frac{1}{m_e^*} + \frac{1}{m_h^*}\right] - \frac{1.8e^2}{4\pi\epsilon\epsilon_0 r} \qquad (7)$$

where 'r' is the radius of the nanoparticle to be calculated, $E_{g(nano)}$ is the bandgap of the nanomaterial, and $E_{g(bulk)}$ is that of bulk material, m_e^* and m_h^* are the effective masses of electron and hole, $\boldsymbol{\varepsilon}$ is the relative permittivity of the material.

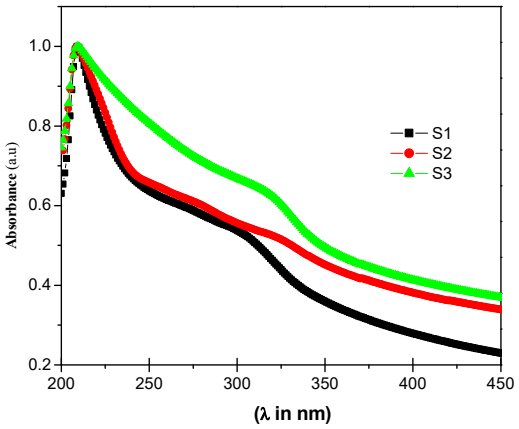

Figure 4. Optical absorption spectra.

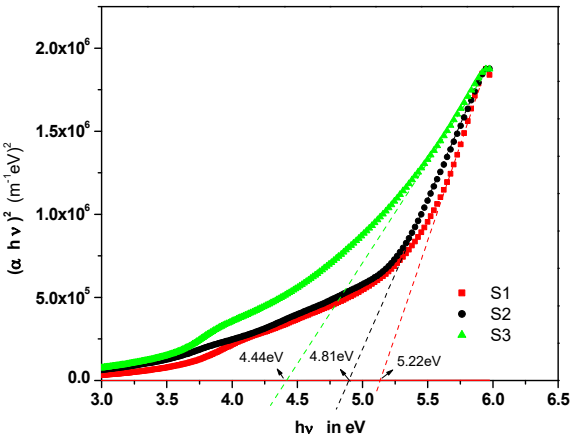

Figure 5. Absorption spectra of as-prepared ZnS thin films, with evidence for direct optical transitions.

Using m_e^* = 0.34m_e and m_h^*= 0.23m_e and $\boldsymbol{\varepsilon}$ = 8.3 for ZnS, the crystallite sizes are calculated as 2.68 nm, 3.1 nm and 3.8 nm for the samples S1, S2 and S3 as summarized in table 3. The difference in the particle size as compared to the particle size obtained from XRD, is because of neglecting second term of the Brus equation while calculating particle size**.**

Photoluminescence Studies

Photoluminescence (PL) corresponds to the light-induced light emission characteristic of the material. Figure 6 illustrates the PL spectrum of ZnS nanoparticles obtained at an excitation wavelength of 350 nm at room temperature. The Photoluminescence spectra show resolved two visible violet light emission bands at 407 nm and 432 nm, which are red, shifted in the visible range. These emissions might be due to defect energy levels present in the ZnS lattice. This violet emission around 407 nm (3.05 eV) can be ascribed to the electron de-excitation from lower level of the conduction band to the valance band of sulphur interstitials. This transition is positioned at nearly 3.05 eV below the CB edge, whereas the

intense violet emission at 432 nm is attributed to transition to Zinc vacancy level from the CB. Similar UV emission is investigated by D. Denzler *et al* [18].

Table 3. Summary of results

sample name	'*t* ' in nm from Ellipsometry	*D* in nm from XRD	*D* in nm using Brus equation	Band edge in nm	E_g in eV	ρ in MΩcm
S1	528.6	4.92	2.68	238	5.20	1.70
S2	575.0	8.56	3.10	258	4.81	10.00
S3	549.4	11.00	3.80	280	4.44	3.64

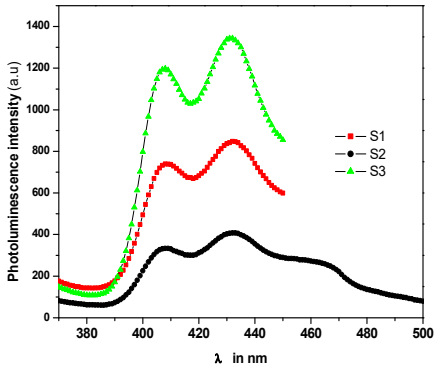

Figure 6. Photoluminescence spectra of ZnS films.

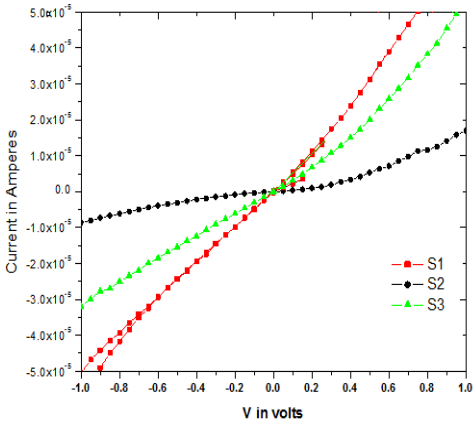

Figure 7. IV characteristics of ZnS thin films.

Ellipsometric studies

Optical constants *n*, *k* and '*t*' the thickness of the film has been determined using the measured values of psi (*Ψ*) and Δ (delta) provided by Ellipsometer in the 200 to 1000 nm range. For the ZnS thin films (S1,S2, and S3 samples) prepared by spin coating, the refractive index values are varying from 1.3 to 1.6, or it is nearly 1.43 as established from the ellipsometric measurements at 632.8 nm and extinction coefficient *k* is

0.398 at 500 nm and peaks at around 400 nm. The thickness of the films estimated as 528.59 nm for S1, 575 nm for S2 and 549.4 nm for S3 film as shown in table 3. These values are used to find the resistivity of the films.

Electric properties

Current-voltage characteristics of the films coated on indium tin oxide glass were obtained by two probe method using Keithley electrometers. Readings were scanned for positive and negative cycles of voltage between -1 to 1V, and corresponding currents were noted. In figure 7, the current-voltage graphs of these films are linear and exhibit ohmic behavior in the voltages measurement range from -1 to +1 volts. Current increases linearly for both positive and negative applied bias up to ±1 volts applied. It is clear from these plots that for voltage of 1V, the current in intrinsic film is of the order of $6x10^{-5}$A. The equation 8, is used to calculate the bulk resistivity of the film,

$$\rho = RA/t \qquad (8)$$

where A is area of cross-section of ohmic contact, ρ is electric resistivity of the film, and 't' is the thickness of the film. From the obtained data and slope of the graphs the resistivity was calculated as 1.7 MΩcm for S1, 10 MΩcm for S2 and 3.64 MΩcm for S3 films which are summarized in table 3. The resistivity values are in agreement with the results reported by other authors [18]. Haque.F *et al.*[17] reported the resistivity of 1.69 x 10^4 Ω cm for the films annealed at 400 °C and $1.73x10^4$ Ω cm for as-deposited films. In case of ZnS thin films prepared by SILAR method[5], *IV* behavior for as-deposited and films annealed at temperatures 100, 150, 200 and 250 °C and the effect of light on *IV* characteristics of films were analyzed. The current

values are about 10^{-10}A, which is less than the current values reported in this paper and these differences in current values are due to change in energy bandgap of ZnS thin film samples.

Conclusions

Zinc sulfide has great potential as a useful material for nanoscale devices due to its non-toxicity and wider bandgap as compared to Cadmium Sulfide (CdS). In this work, wide bandgap and conducting ZnS nanocrystals are obtained by simple co-precipitation method using low-cost precursors without using any capping agent at different precursor concentrations. The influence of sulphur concentration on structural, optical, and electronic properties is found to be considerable and important. Metal to sulfide ratio has been shown to have a significant effect on the number of zinc ions precipitated from solution and hence on the particle size. X-ray diffraction reveals the polycrystalline nature of material with cubic phase and particle size of 4.92 nm, 8.56 nm, and 11 nm. The optical absorption studies reveal a large blue shift of the absorption edge from their bulk values resulting from quantum confinement effect. The optical band gap decreases as the sulphur concentration in the reaction mixture increases. As obtained ZnS films show promise for applications in high frequency UV detectors and other optoelectronic devices.

Acknowledgements

This work is supported by K.L.E Technological University under “Capacity building projects” grants. The authors thank to the management of K.L.E Technological University, Hubballi for providing financial support

References

1. Sarute, U.; Yingyot, I. A comprehensive review on ZnS: From synthesis to an approach on solar cell, *Renew. Sust. Energ. Rev.* **2016**, *55*, 17-24.

2. Konstantatos, G.; Sargent, E. H. *Colloidal Quantum Dot Optoelectronics and Photovoltaics,* Cambridge University Press, UK, 2013.

3. Fang, X.; Zhai, T.; Gautam, U. K.; Li,L.; Wu, L.; Bando, Y.; Golberg, D. ZnS nanostructures: From synthesis to applications. *Prog. Mater. Sci.* **2011**, *56*, 175-287.

4. Fang, X.; Bando, Y.; Gautam, U. K.; Zhai, T.; Zeng, H.; Xu, X.; Liao, M.; Golberg, D. ZnO and ZnS Nanostructures: Ultraviolet-Light Emitters, Lasers and Sensors. *Crit. Rev. Solid State Sci.* **2009**, *34*, 190-223.

5. Ates, A.; Yildirım, M. Ali.; Kundakci, M.; Astam, A. Annealing and light effect on optical and electrical properties of ZnS thin films grown with the SILAR method. *Mater. Sci. Semicond. Process.* **2007**, *10*, 281-286.

6. Gangopadhyay, U.; Kim, K.; Mangalaraj, D.; Yi, J. *Low-cost CBD ZnS* antireflection coating on large area commercial mono-crystalline silicon solar cells. *Appl. Surf. Sci.* **2004**, *230*, 364-370.

7. Bindu, K. R.; Sreenivasan, P. V.; Martinez, A. I.; Anila, E. I. a-Axis oriented ZnS thin film synthesised by dip-coating method. *J. Sol-Gel Sci. Technol.* **2013**, *68*, 351-355.

8. Ummartyotin, S.; Bunnak, N.; Juntaro, J.; Sain, M.; Manuspiya, H. Synthesis and luminescence properties of ZnS and metal (Mn, Cu)-doped-ZnS ceramic powder. *Solid State Sci.* **2012**, *14*, 299-304.

9. Goktas, A.; Aslan, F.; Yasar, E.; Mutlu, I. H. Preparation and characterisation of thickness-dependent nano-structured ZnS thin films by sol-gel technique. *J. Mater. Sci.: Mater. Electron.* **2012**, *23*, 1361.

10. Firoozifar, S. A. R.; Behjat. A.; Kadivar, E.; Ghorashia, S. M. B.; Zarandia, M. B. A study of the optical properties and adhesion of zinc sulfide anti-reflection thin film coated on a germanium substrate. *Appl. Surf. Sci.* **2011**, *258*, 818-821.

11. Tec-Yam, S.; Rojas, J.; Rejon, V.; Oliva, A. I. High-quality anti-reflective ZnS thin films prepared by chemical bath deposition. *Mater. Chem. Phys.* **2012**, *136*, 386-393.

12. Yoo, D.; Choi, M. S.; Heo, S. C.; Chung, C.; Kim, D.; Choi, C. Structural, Optical and Chemical Analysis of Zinc Sulfide Thin Film Deposited by RF-Magnetron Sputtering and Post Deposition Annealing. *Met. Mater. Int.* **2013**, *19*, 1309-1316.

13. Kole, A. K.; Kumbhakar, P. Cubic-to-hexagonal phase transition and optical properties of chemically synthesized ZnS nanocrystals. *Results Phys.* **2012**, *2*, 150-155.

14. Saleem, M.; Fang, L.; Wakeel, A.; Rashad, M.; Kong, C. Y. Simple Preparation and Characterization of Nano-Crystalline Zinc Oxide Thin Films by Sol-Gel Method on Glass Substrate. *World J. Condens. Matter. Phys.* **2012**, *2*, 10-15.

15. Lewis, A. E. Review of metal sulphide precipitation. *Hydrometallurgy* **2010**, *104*, 222-234.

16. Hoa, T. T. Q.; Vu, L. V.; Canh, T. D.; Long, N. N. Preparation of ZnS nanoparticles by hydrothermal method. *Phys.: J. Phy. Conf. Ser.* **2009**, *187*, 012081.

17. Haque, F.; Rahman, K. S.; Islam, M. A.; Rashid, M. J.; Akhtaruzzaman, M.; Alam, M. M.; Alothman, Z. A.; Sopian, K.; Amin, N. Growth optimization of ZnS thin films by rf magnetron sputtering as prospective buffer layer in thin-film solar cells. *Chalcogenide Lett.* **2014**, *11*, 189-197.

18. Denzler, D.; Olschewski, M.; Sattler, K. Luminescence studies of localized gap states in colloidal ZnS nanocrystals. *J. Appl. Phys.* **1998**, *84*, 2841-2845.